Ci 81

UDC 556.16:519.876.5

ACTA POLYTECHNICA SCANDINAVICA

CIVIL ENGINEERING AND BUILDING CONSTRUCTION SERIES NO. 81

Adaptive Rainfall-Runoff Model, SATT-I

PERTTI VAKKILAINEN

Helsinki University of Technology
Laboratory of Hydrology and Water Resources Engineering
SF-02150 Espoo 15, Finland

TUOMO KARVONEN

Finnish Drainage Centre
Simonkatu 12 A 11
SF-00100 Helsinki 10, Finland

HELSINKI 1982

Ci 81

UDC 556.16:519.876.5

A C T A

P O L Y T E C H N I C A

S C A N D I N A V I C A

Civil Engineering and Building Construction Series No. 81

Adaptive Rainfall-Runoff Model, SATT-I

Pertti Vakkilainen

Helsinki University of Technology
Laboratory of Hydrology and Water Resources Engineering
SF-02150 Espoo 15, Finland

Tuomo Karvonen

Finnish Drainage Centre
Simonkatu 12 A 11
SF-00100 Helsinki 10, Finland

HELSINKI 1982

Vakkilainen, P. and Karvonen T.: Adaptive Rainfall-Runoff Model, SATT-I. Acta Polytechnica Scandinavica, Civil Engineering and Building Construction Series No. 81, Helsinki 1982, 54 pp. ISBN 951-666-151-3. ISSN 0355-2705.

ABSTRACT

The rainfall-runoff model SATT-I is introduced. In the model soil moisture can be treated in a physically based or in a conceptual way. Similarly, flood routing can be calculated either by using St. Venant's equations or by using the Muskingum method. The latter is also used in the timing of direct runoff. The regulation routines for lakes and reservoirs are versatile and applicable to all practical cases. The model has 10 calibrable parameters whose values can be searched with an automatic calibration using the siplex algorithm. The model is provided with an adaptive calibration system which improves the accuracy of forecasts as new data are available. After presentation of the model some practical applications to the Kyrönjoki river basin in Western Finland are given.

CONTENTS

1 INTRODUCTION

The low intensity of rainfall, the peak discharges caused by melt water, and the freezing of soil constitute the most essential hydrological factors due to the climate in Finland. The great number of lakes (9.4 % of the country's area), the vast forest areas (71 %), the orographic uniformity of the ground and the predominance of morainic soil are the main geomorphological features which condition the movement of water in a typical Finnish catchment basin. In Finland, hydrological interrelations have traditionally been analysed with the aid of statistical methods. The first rainfall-runoff model developed in Finland was worked out by Virta /38/. In the National Board of Waters studies have been carried out /18, 19/ on the applicability of the HBV model developed by Bergström /5/. Vakkilainen & Karvonen /37/ and Karvonen /14/ have studied the use of the SSARR model in a research programme which also involved the application of linear rainfall-runoff and snowmelt-runoff models /35/. The idea of developing a new model applicable to Finnish conditions emerged during these investigations. At the same time, Salaojakeskus (Finnish Drainage Centre) discussed the methods available for improved drainage performance; one of the conclusions was that subsurface drainage would work better in many places if only the high-water stages in nearby watercourses could be appropriately evened out by means of well-timed filling of flood control reservoirs. The joint investigations carried out upon these approaches resulted in the Finnish rainfall-runoff model SATT-I (Fig. 1).

While developing the SATT-I model the goal was to create a computer model program which would fulfil the following requirements:

- applicability to all kinds of watercourses;
- simplicity of use with the possibility to run the program in both timesharing and batch processes;
- suitability for processing on both large and small computers;

- the required input data consist of observations logged on generally measured hydrological variables: precipitation, temperature, water equivalent of snow, groundwater level, discharge, evaporation from the Class A pan;
- the evaluation of soil moisture content is based on physical principles;
- the model is suited for both the forecasting of streamflow discharge and the evaluation of various effects caused by river regulation and water engineering schemes;
- the accuracy of forecasts must continually improve as new cumulative data are entered;
- the computing routines related to the regulation of flood reservoirs should be as versatile as possible.

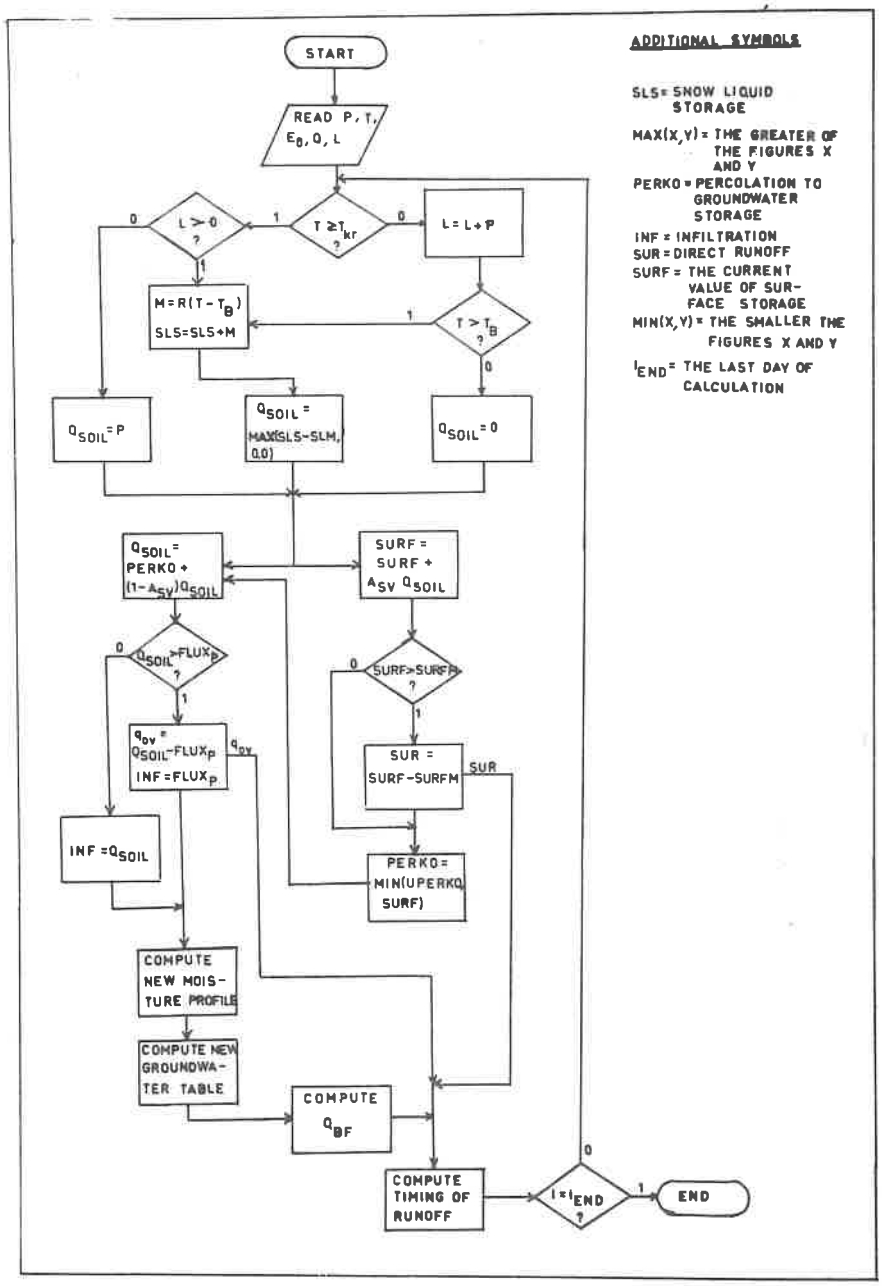

Figure 1. SATT-I model.

2 DESCRIPTION OF THE MODEL

2.1 Precipitation and snowmelt

During the calibration stage, a weight coefficient is determined for each precipitation gauging station for the calculation of areal precipitation. The form of precipitation (water vs. snow) is tested on the basis of daily mean temperatures. When the daily mean temperature is above a critical temperature (T_{kr}) (entered as input data) precipitation is considered as rainfall and in the opposite case as snowfall; in this latter case, an increase is registered in the water equivalent of snow cover. The value of T_{kr} is obtained through calibration. Generally it is between 0.0 to 1.2°C.

The rate of snowmelt is calculated by means of base temperature (T_B) and a parameter of snowmelt rate (R) using the following formula (1) (e.g. /33/):

$$M = R\ (T - T_B), \qquad (1)$$

where

M is snowmelt rate (mm/d)
R snowmelt rate parameter (mm/°C/d)
T mean daily temperature (°C)
T_B base temperature (°C)

The melting of snow does not always cause an increase in the amount of water released from the snow cover since melt water can be retained in it. Runoff may result only if the snow has reached its water saturation point (SLM), which generally falls between 5 to 15 per cent of the respective water equivalent. The maximum water retention capacity SLM can be determined by calibration.

Melting normally causes the snow cover to disappear unevenly from the catchment area. No practicable data are available on the proportions of naked and covered ground during the melting period. In the SATT-I model the decrease of snow-

covered area is taken into account through the water equivalent of snow according to Fig. 2. When the water equivalent falls below a calibrated limit value (L_{limit}), catchment area gradually becomes exposed from beneath the snow cover. The decrease coefficient (K_v) is determined from the formula

$$K_v = (L/L_{limit})^{1.5} \text{ , when } L < L_{limit}, \qquad (2)$$

where

K_v is a decrease coefficient which indicates the proportion of snow-covered area ($K_v = 1.0$ when $L \geq L_{limit}$)
L areal value of the water equivalent of snow (mm)
L_{limit} limit value for the water equivalent of snow (mm)

If the value of K_v evaluated from formula (2) falls below 0.10, it is then assigned the value 0.10. This is done in order to permit the water equivalent of snow finally to diminish to zero.

The effective snowmelt rate (M_T) can then be obtained as the product of K_v and the snowmelt rate M from formula (1):

$$M_T = K_v \cdot M \qquad (3)$$

2.2 Evapotranspiration

The amount of potential evaporation from the ground can be determined according to the methods discussed by Vakkilainen /36/. Thus, when using evaporation data from a Class A pan, the following formula is used:

$$E_p = (0.05 + 0.18 \ln t)\, E_o, \qquad (4)$$

where

E_p is potential evaporation (mm/d)
E_o evaporation from the Class A pan (mm/d)
t time (days) from the beginning of May

The actual evaporation is evaluated as the product of potential evaporation and a coefficient (α) which depends on the matric potential of the root zone as shown in Fig. 3.

Vegetation retains a portion of precipitation by interception. This interception storage is exposed to potential evaporation. The coverage coefficient (cc) indicates the proportion of catchment area on which interception occurs. Only that portion of precipitation which exceeds the sum of maximum interception storage (STO) and E_p, can reach the ground. The value of STO is a calibrated parameter. The SATT-I model also permits consideration of interception storage as part of surface storage (Fig. 1).

Evaporation occurring from the surface of snow is supposed to be dependent on temperature in the following way:

- when $T \geq 1.0\ ^{o}C$, $E_s = 0.2$ mm/d
- when $-1.0 \leq T < 1.0$, $E_s = 0.3$ mm/d
- when $T < 1.0$, $E_s = 0.1$ mm/d

These values coincide with experimental data on evaporation from snow as reported by Kaitera & Teräsvirta /13/.

The evaporation which occurs from the snow-free areas during the melting period is taken into account by reducing the rate of snowmelt by the amount E_v:

$$E_v = (1 - K_v)\ E_p, \qquad (5)$$

where

E_v is evaporation from the snow-free portion of catchment area (mm/d)

2.3 Soil moisture

2.31 Option No. 1

The principle:

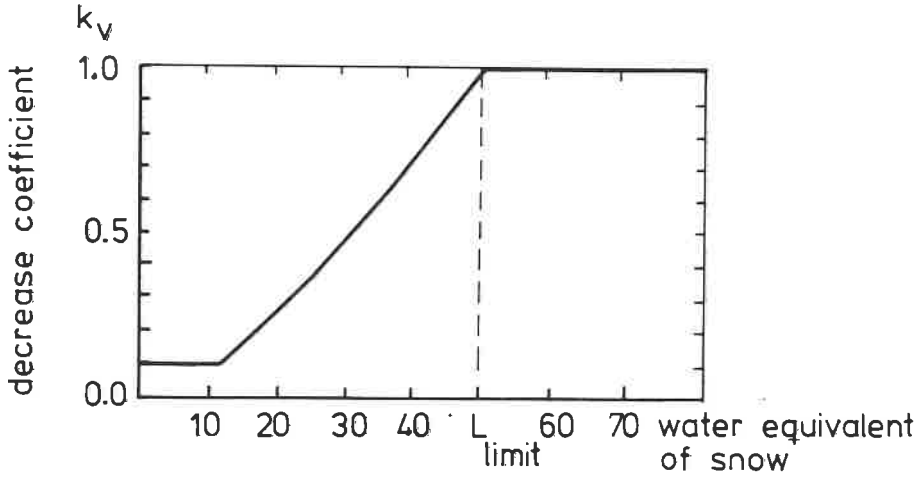

Figure 2. Decrease of snow-covered area as a function of water equivalent of snow.

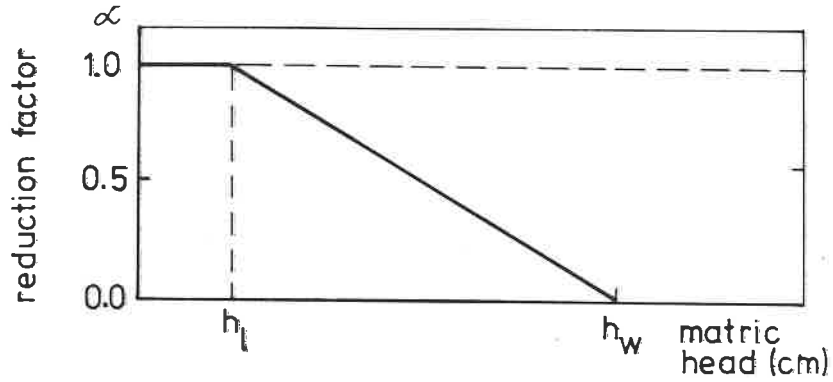

Figure 3. Reduction factor (α) for potential evaporation as a function of matric head.

The vertical movement of soil water can be simulated by equations (6) and (7) (e.g. /9/):

$$q = K(h) \left(\frac{\partial h}{\partial z} + 1\right) \tag{6}$$

$$\frac{\partial h}{\partial t} = \frac{1}{C(h)} \left(\frac{\partial q}{\partial z} - r\right) \tag{7}$$

where

q is flux (cm/d)
K hydraulic conductivity (cm/d)
h matric head (cm)
z vertical distance from soil surface (cm)
t time (days)
r volume of water going from or to the profile
C differential water capacity

These equations are solved according to an implicit procedure as follows:

$$q_{i,n+1} = K_{i+\frac{1}{2},n} \left(\frac{h_{i+1,n+1} - h_{i,n+1}}{\Delta z} + 1\right) \tag{8a}$$

$$q_{i,n+1} = K_{i-\frac{1}{2},n} \left(\frac{h_{i,n+1} - h_{i-1,n+1}}{\Delta z} + 1\right) \tag{8b}$$

$$\frac{1}{\Delta t} (h_{i,n+1} - h_{i,n}) = \frac{-1}{C(h_{i,n})} \frac{1}{\Delta z} (q_{i,n+1} - q_{i-1,n+1} - r_{i,n}) \tag{9}$$

where

$$K_{i+\frac{1}{2},n} = \sqrt{K_{i+1,n} \cdot K_{i,n}}$$

$$K_{i-\frac{1}{2},n} = \sqrt{K_{i,n} \cdot K_{i-1,n}}$$

i is nodal point of depth
n nodal point of time
Δz depth increment
Δt time increment

Combining equations (8) with equation (9), the latter can be

expressed as a set of linear equations (10):

$$A_i h_{i+1,n+1} + B_i h_{i,n+1} + D_i h_{i-1,n+1} = E_i \qquad (10)$$

where

$$A_i = - \frac{\Delta t}{C(h_{i,n})\ \Delta z} K_{i+\frac{1}{2},n} \qquad (11)$$

$$D_i = - \frac{\Delta t}{C(h_{i,n})\ \Delta z} K_{i-\frac{1}{2},n} \qquad (12)$$

$$B_i = 1 - A_i - B_i \qquad (13)$$

$$E_i = h_{i,n} + \frac{\Delta t}{C(h_{i,n})\ \Delta z} (K_{i+\frac{1}{2},n} - K_{i-\frac{1}{2},n} - r_{i,n}) \qquad (14)$$

The upper boundary condition at the point i = 1 is the so-called Neumann's condition which defines the flux to the nodal point by the following equations (15) and (16):

$$q_{1,n+1} = Q_{soil}, \quad \text{when} \quad Q_{soil} \leq FLUX_p \qquad (15a)$$

$$q_{1,n+1} = FLUX_p, \quad \text{when} \quad Q_{soil} > FLUX_p \qquad (15b)$$

$$FLUX_p = K_{1-\frac{1}{2},n} \left(\frac{h_{1,n} - h_{0,n}}{0.5\ z_p} + 1\right) \qquad (16)$$

where (cf. Fig. 4):

$q_{1,n+1}$ is flux to nodal point i = 1
Q_{soil} quantity of incident water on soil surface
$FLUX_p$ maximum possible infiltration
$h_{1,n}$ matric head (cm) at point i = 1
$h_{0,n}$ matric head (cm) at soil surface
z_p thickness of top soil layer (cm)

At nodal point i = 1, equations (11)...(14) become

$$A_1 = - \frac{\Delta t}{C(h_{1,n})\ \Delta z_1} K_{1+\frac{1}{2},n} \qquad (17)$$

$$D_1 = 0.0 \qquad (18)$$

$$B_1 = 1 - A_1 \qquad (19)$$

$$E_1 = h_{1,n} + \frac{\Delta t}{C(h_{1,n})} \frac{1}{z_p} (K_{1+\frac{1}{2},n} - q_{1,n+1} - r_{1,n}) \quad (20)$$

The lower boundary condition is of the so-called Dirichlecht type. At the first nodal point N above ground-water table the matric head has the value $h_{N,n+1}$ which is equal to the distance of this point from the ground-water table.

Equations (10)...(14) and (17)...(20) can be expressed in the matrix form as follows:

$$\begin{bmatrix} B_1 & A_1 & 0 & \cdot & 0 \\ D_2 & B_2 & A_2 & \cdot & \cdot \\ 0 & D_3 & B_3 & A_3 & \cdot \\ \cdot & \cdot & \cdot & \cdot & \cdot \\ \cdot & \cdot & \cdot & \cdot & \cdot \\ 0 & \cdot & D_{N-1} & B_{N-1} & A_{N-1} \end{bmatrix} \begin{bmatrix} h_{1,n+1} \\ h_{2,n+1} \\ \cdot \\ \cdot \\ \cdot \\ h_{N-1,n+1} \end{bmatrix} = \begin{bmatrix} E_1 \\ E_2 \\ \cdot \\ \cdot \\ \cdot \\ E_{N-1} \end{bmatrix} \quad (21)$$

Equation (21) is solved with the aid of the so-called Thomas algorithm, an application of Gauss' elimination technique /30/.

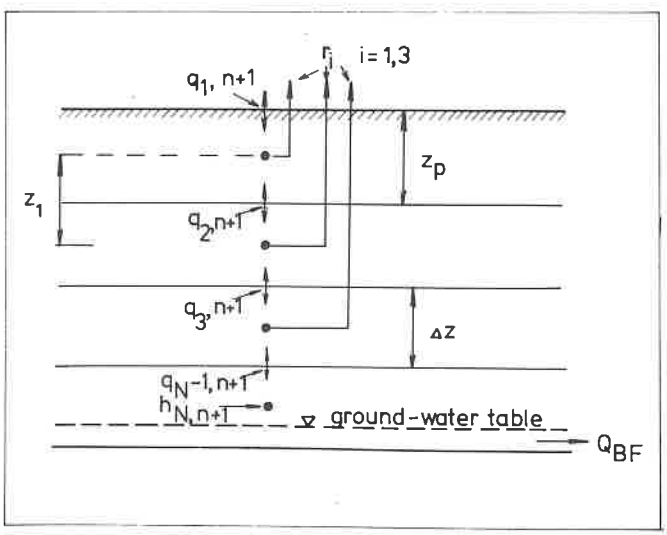

Figure 4. The principle of soil moisture accounting for option No. 1.

Values of the sink term r are evaluated in the following way:

$$ROOT = z_p + 2\,\Delta z \tag{22}$$

$$r_{i,n} = -\alpha_i\, E_p \tag{23}$$

$$\alpha_i = \frac{z_p}{ROOT}\,\frac{h_w - h_{i,n}}{h_w - h_\ell} \tag{24}$$

where

ROOT is estimated depth of the root layer (cm)
z_p thickness of the topsoil layer (cm)
α reduction factor for potential evaporation (Fig. 3)
h_w matric head at wilting point (Fig. 3)
h_ℓ matric head at the limiting point (Fig. 3)

A water retention curve and the values of hydraulic conductivity are needed for the calculation. These can be estimated to a fair degree of accuracy, provided that sufficient data are available on soil conditions in the catchment area (e.g. /3,4/). If necessary, both the water retention curve and the values of hydraulic conductivity can be calibrated appropriately. Interrelations characteristic to some soil types are shown in Fig. 5 and in Fig. 6.

Evaluation of ground-water level

The evaluation of ground-water level is based on the use of water balance and the differential water capacity. Once the values of the matric potential $h_{i,n+1}$ attached to the moment n+1 have been determined as shown before, the change in the water content of the soil profile is calculated from the following equation:

$$\Delta S = S_{n+1} - S_n - E_a + q_{1,n+1} - Q_{BF} \tag{25}$$

where

ΔS is change in the water content of the profile (mm)

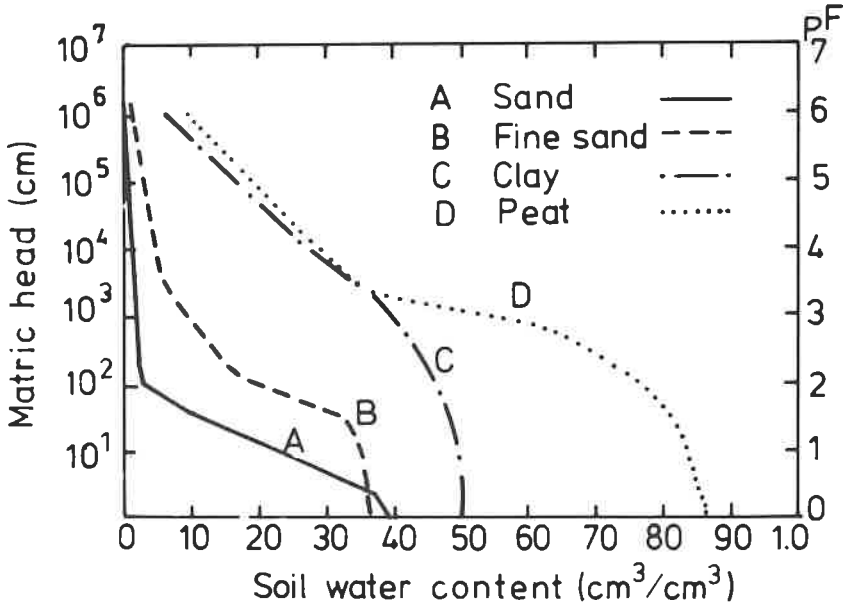

Figure 5. Matric head as a function of soil water contents for 4 different soils.

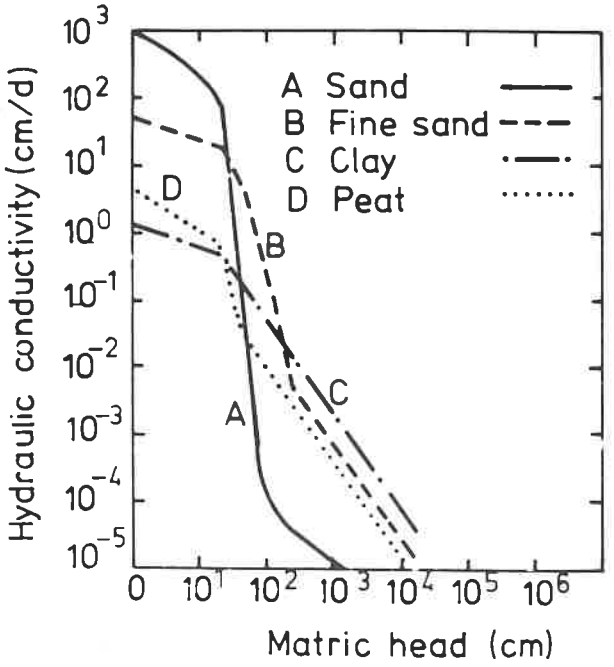

Figure 6. Hydraulic conductivity as a function of matric head for 4 different soils.

S_n is water content (mm) of the profile at the moment n
S_{n+1} water content (mm) of the profile at the moment n+1
E_a actual evaporation (mm) (from equation (23))
$q_{1,n+1}$ flux (mm) to nodal point i = 1
Q_{BF} base flow (mm)

The amount of base flow is evaluated from the values of ground-water level according to /4/:

$$Q_{BF} = a_1 \, e^{- b_1 \, GWL}, \tag{26}$$

where

a_1, b_1 are empirical coefficients determined during model calibration stage from data on ground-water level and discharge
GWL is distance from soil surface to ground water table (cm)

The term ΔS in equation (25) stands for water flux from ground-water into the non-saturated zone. The term DIF is formed for the calculation of ground-water level and it is summed with ΔS after each time step:

$$DIF = DIF + \Delta S \tag{27}$$

When $|DIF|$ > limit value (= 1.0...1.5 mm) the program will evaluate the change in ground-water level from the equation

$$\Delta GWL = \frac{DIF}{\Delta Z \; C_R \; (N-1)} \tag{28}$$

where

ΔGWL is change in ground-water level
C_K differential water capacity in saturated soil
N number of nodal points above ground-water table

Once the change in ground-water level has been determined, the moisture profile of the soil body is modified accordingly:

$$\Delta h_{i,n+1} = \frac{-DIF}{\Delta Z \; C(h_{i,n+1}) \; (N-1)} \; ; \; i = 2,N \qquad (29)$$

where

$\Delta h_{i,n+1}$ is change in matric potential at point i

Frost

In order to take into account the effect of frost on the perviousness of soil, two variables V_{min} and F_S are included in the model. When part of the soil is frozen, the value of hydraulic conductivity K_R is calculated from the following equations:

$$K_R = K_{REL} \cdot K \qquad (30)$$

$$K_{REL} = \frac{(D_S - D_F)}{D_F}(1-V_{MIN}) - V_{MIN} \qquad (31)$$

$$D_F = D_{F-1} - F_S \qquad (32)$$

where

K_R is actual hydraulic conductivity (cm/d)
K_{REL} relative hydraulic conductivity (cm/d)
K hydraulic conductivity of non-frozen soil (cm/d)
V_{MIN} ratio between the minimum hydraulic conductivity of frozen soil and the hydraulic conductivity of non-frozen soil
D_S initial depth of frost (cm)
D_F current depth of frost (cm)
D_{F-1} depth of frost (cm) on the previous day
F_S change in frost depth (cm)

The value of V_{MIN} is determined as explained in paragraph 3.2. The depth of frost is reduced by the following average values given by Keränen /15/:

- sandy and moraine soils 2.7 cm/d
- clayey soils 1.6 cm/d
- peat soils 0.9 cm/d
- cultivated soil 2.0 cm/d

If the soil is still covered in snow, then $F_s = 0$.

2.32 Option No. 2

If data on ground-water level are not available for the catchment area under consideration, the evaluation of ground-water stages explained in option 1 must be omitted. The rest of the procedure for the determination of soil moisture remains unchanged. Fluctuations in ground-water level are replaced by those occurring in ground-water storage. The method for the calculation of the base flow from this storage is explained in paragraph 2.42.

The principle of option 2 is shown in Fig. 7.

2.33 Option No. 3

In this option, the whole of the non-saturated zone is considered alone as a single layer; the calculation of soil moisture can thus be carried out simply on the basis of water budget. The amount of water entering the soil is calculated from equations (15) and (16) as previously. The amount of water percolatig into ground-water storage is determined from equation (6). The base flow is again evaluated as explained in paragraph 2.42.

The principle of option 3 is shown in Fig. 8.

2.4 Runoff

2.41 Formation of runoff

According to the traditional theory formulated by Horton, floods are due to overland flow occurring in the whole of the catchment area. The theory states that overland flow occurs as soon as the amount of precipitation and/or snowmelt rate exceed the infiltration capacity of the soil.

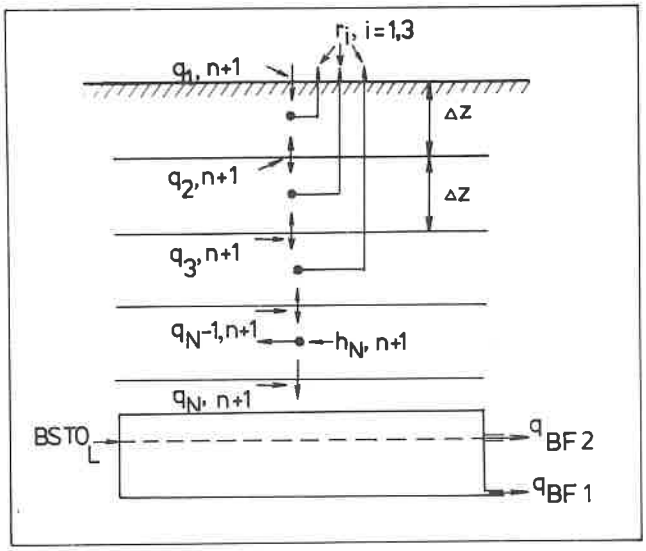

Figure 7. The principle of soil moisture accounting for option No. 2.

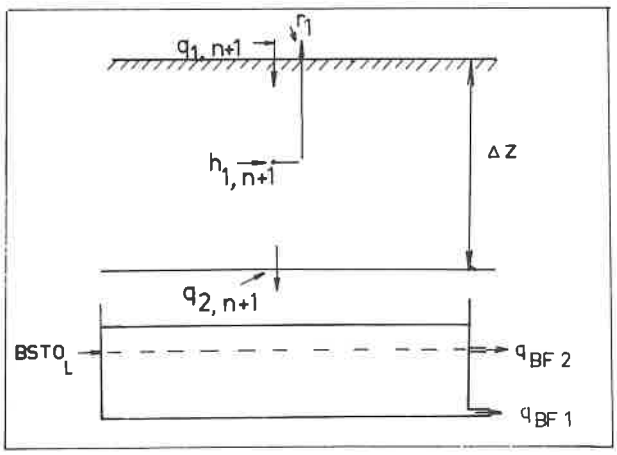

Figure 8. The principle of soil moisture accounting for option No. 3.

However, the actual process of formation of runoff probably differs essentially from Horton's theory especially in humid climate. In Finland, the low intensities of rainfall create a situation where, particularly in summertime, the infiltration capacity of soil is greater than the intensity of rainfall. An exception to this are the clayey lands under cultivation where, once the arable topsoil layer has reached saturation, part of the precipitation may be turned into surface runoff which is collected by the drainage network (partial area overland flow). In addition to this, springtime frost may cause surface runoff originating in melt water released from snow.

Various studies carried out in different parts of the world have made it clear that ground-water generally accounts for a considerable part of flood discharge /8, 23, 31, 32/. According to these studies, 50 to 90 per cent of the total discharge during flood periods originates from ground-water. In other words, only 10 to 50 per cent of the total discharge is due to precipitation and snowmelt occurred during flood period under consideration. In the physical sense, the runoff from ground-water is constituted by "old" water, i.e. from snowmelt and rain water infiltrated into the ground during preceding years.

The studies mentioned above are based on the use of natural environmental isotopes - mainly ^{18}O, deuterium, tritium - as tracers. The concentration of the traced isotope in the ground-water differs essentially from its concentration in snowmelt and rainfall water. The proportion of total flood-time discharge due to ground-water can be determined from equations (33) and (34) /32/:

$$Q_t = Q_p + Q_s \tag{33}$$

$$C_t Q_t = C_p Q_p + C_s Q_s \tag{34}$$

where

Q is discharge
C tracer concentration

t is sub-index denoting total discharge
p sub-index denoting ground-water
s sub-index denoting snowmelt and rainfall water

The above equations have two unknown quantities Q_p and Q_s. The other quantities can be measured, for instance, once a day. The value for C_p is brought forward from the period immediately preceding the flood and during which all runoff may be assumed to consist of base flow.

So far, it has been impossible to give an explicit reason for the process which can result in floods where as much as 90 per cent of total discharge is produced by slowly-moving ground-water. One possible theory is that infiltration from rainfall and snowmelt causes the ground-water table to rise very near the soil surface in the vicinity of rivers and streams. This kind of massive infiltration, as it were, pushes the old water out of the soil. The longer the infiltration goes on, the larger will be the area from which ground-water is released into open water channels. Those areas where the ground-water is very near the surface can also produce surface runoff (variable source area - overland flow).

2.42 Designing a model for runoff

The SATT-I program is aimed at representing the above theory of runoff by a model which is based on empirical mathematical equations and the soil-vegetation-atmosphere system discussed in Chapter 2.

Those parts of the catchment area which have poor hydraulic conductivity or which are completely impervious are treated separately in the SATT-I program (these areas consist mainly of clayey soils and some lakes which are omitted in the calculations). The size of the active water storage is determined for these partial areas by calibration. This surface storage must be filled before overland runoff can occur. The amount of the storage generally fluctuates between 10 and 50 mm, and it works as a buffer which retains even heavy

summertime rainfall so that no runoff can take place. The surface storage is exposed to evaporation at the potential level, and part of it percolates into the non-saturated soil zone.

That portion of precipitation and snowmelt (=1 - A_{SV} , where A_{SV} represents the poorly conductive or impervious proportion of catchment area) which is not retained in the surface storage may cause overland runoff if the hydraulic conductivity of the soil is essentially reduced by frost. The maximum possible infiltration can be determined from formula (16), and the actual infiltration is evaluated from equation (15). The proportion q_{ov} of overland runoff from the pervious parts of the catchment area can be expressed by the following equations:

$$q_{ov} = \begin{cases} 0.0 & , \text{ when } Q_{soil} \leq FLUX_p \\ Q_{soil} - FLUX_p & , \text{ when } Q_{soil} > FLUX_p \end{cases} \quad (35)$$

$$Q_{soil} = (1-A_{SV}) \ (P_a+M_t) \quad (36)$$

where

q_{ov} is overland runoff
$FLUX_p$ maximum possible infiltration
A_{SV} proportion of poorly conductive or impervious area in the catchment area
P_a areal precipitation
M_t actual amount of snowmelt

In option 1, the base runoff is calculated from formula (26). The coefficients a_1 and b_1 are determined by calibration; a close guess can be found on the basis of summer low water stages if the respective data on ground-water level are available.

In model versions 2 and 3, the base runoff is calculated from the current amount of ground-water storage. Initially it

was assumed that this storage changes in a linear manner. However, various processings of the data on computer with automatic calibration showed that a considerably better result can be obtained if the value of the storage is raised to the power 1.3:

$$q_{BF1} = a\ BSTO^{1.3} \tag{37}$$

where

q_{BF1} is discharge from ground-water storage
a coefficient
BSTO size of ground-water storage at the beginning of the time step considered

We have stated in paragraph 2.42 that base runoff may also have an important role in causing high-water stages. To design a physically reliable model for the rapid discharge occurring from the ground-water storage would make it necessary to use a three-dimensional approach. Satisfactory results can however be reached by modifying the mode of discharge from the ground-water storage when the value of BSTO exceeds a certain limit value $BSTO_L$. In a physical interpretation this means that $BSTO_L$ can be assumed to represent the break-point at which the ground-water table has reached a level which is very close to soil surface in the vicinity of open water channels. As BSTO increases further, the area from which base runoff is released to the channels grows larger.

$$q_{BF2} = \begin{cases} 0.0 & \text{, when } BSTO \leq BSTO_L \\ b\ (BSTO - BSTO_L)^{1.3} & \text{, when } BSTO > BSTO_L \end{cases} \tag{38}$$

where

q_{BF2} is discharge from ground-water storage
BSTO size of ground-water storage at the beginning of the time step considered
$BSTO_L$ limit size of ground-water storage
b coefficient

2.43 Timing of direct runoff

The calculation procedure used in SATT-I for the timing of direct runoff is the so-called Muskingum's method which has its most general application in the calculation of flood-wave propagation in rivers. The method can also be applied to the calculation of runoff peak advance in a catchment area. Testing the SATT-I program proved that the Muskingum method is more appropriate for the model structure chosen than the procedure used in the SSARR model in which the runoff components are conveyed through a series of 3 to 5 successive linear reservoirs /34/.

The following equations are used in the Muskingum method /28/:

$$Q_{j+1}^{n+1} = C_1 Q_j^n + C_2 Q_j^{n+1} + C_3 Q_{j+1}^n \tag{39}$$

$$C_1 = \frac{t/k + 2X}{t/k + 2(1-X)} \tag{40}$$

$$C_2 = \frac{t/k - 2X}{t/k + 2(1-X)} \tag{41}$$

$$C_3 = \frac{2(1 - X) - t/k}{t/k + 2(1-X)} \tag{42}$$

where

Q_{j+1}^{n+1}	is	calculated discharge at the end of the time step considered
Q_j^n		incoming discharge at the beginning of the time step considered
Q_j^{n+1}		incoming discharge at the end of the time step considered
Q_{j+1}^n		calculated discharge at the beginning of the time step considered
t		length of the time step
k		distance between the centres of gravity of the incoming discharge and the calculated discharge
X		shape factor

2.5 Flood routing

2.51 Channel routing by the implicit method

The equations for unsteady flow consisting of the equations for the conservation of mass and momentum are a very powerful analytical tool for the study of such problems as surface runoff, surges in canals, reservoir regulation and flood movements. Considerable activity aimed at finding numerical solutions of the complete equations has taken place during the last 10-15 years (e.g. /1, 2, 11, 20, 21/).

The desirability of using large time steps in computations has led to the development of implicit methods. In the SATT-I model the so-called Preissmann-scheme has been selected. The equations of unsteady flow in open channels can be expressed in the form (e.g. /7/):

$$b \frac{\partial y}{\partial t} + \frac{\partial Q}{\partial x} - q = 0 \tag{43}$$

$$\frac{\partial Q}{\partial t} + \frac{\partial}{\partial x}\left(\beta \frac{Q^2}{A}\right) + gA\left(\frac{\partial y}{\partial x} + S_f\right) - v_x q = 0 \tag{44}$$

$$S_f = \frac{n^2 Q^2}{A^2 R^{4/3}} \tag{45}$$

where

- x is distance in the positive direction
- t time
- y stage above a fixed datum
- Q discharge
- b water surface top width of the channel
- q lateral flow per unit length along the channel, positive if it is inflow
- A cross-sectional area of flow
- β momentum correction factor
- g acceleration due to gravity
- S_f resistance slope, given by (45)
- n Manning roughness coefficient
- R hydraulic radius

Equations (43) and (44) make up a system of two nonlinear first-order first-degree partial differential equations of the hyperbolic type. They have two independent variables x and t and two dependent variables y and Q. The other terms are either known functions of x, t , y and Q or they are constants. No analytical solutions are presently known. The equations can be solved, however, by writing them in finite difference form and using a digital computer to perform numerical computations required.

Consider a nonuniform rectangular grid on the x, t plane, as shown in Fig. 9. Distances along the channel are represented by abscissas and times are represented by ordinates. The partial derivatives at a point M, are expressed as follows:

$$\frac{\partial f}{\partial t} = \frac{1}{2\Delta t}\left(f_{i+1}^{j+1} - f_{i+1}^{j} + f_{i}^{j+1} - f_{i}^{j}\right) \tag{46a}$$

$$\frac{\partial f}{\partial x} = \theta\frac{f_{i+1}^{j+1} - f_{i}^{j+1}}{\Delta x} + (1-\theta)\frac{f_{i+1}^{j} - f_{i}^{j}}{\Delta x} \tag{46b}$$

where

f is the variable, y or Q

θ weighting factor

The coefficients of equations (43) and (44), when presented according to the Preissmann formulation

$$f(x,t) = \frac{\theta}{2}\left(f_{i+1}^{j+1} + f_{i}^{j+1}\right) + \frac{(1-\theta)}{2}\left(f_{i+1}^{j} + f_{i}^{j}\right) \tag{47}$$

yield together with the derivatives expressed by equations (46a) and (46b), two algebraic equations:

$$\frac{1}{2\Delta t}\hat{b}\left(y_{i+1}^{j+1} - y_{i+1}^{j} + y_{i}^{j+1} - y_{i}^{j}\right) + \frac{\theta}{\Delta x}\left(Q_{i+1}^{j+1} - Q_{i}^{j+1}\right)$$

$$+ \frac{(1-\theta)}{\Delta x}\left(Q_{i+1}^{j} - Q_{i}^{j}\right) - \hat{q} = 0 \tag{48a}$$

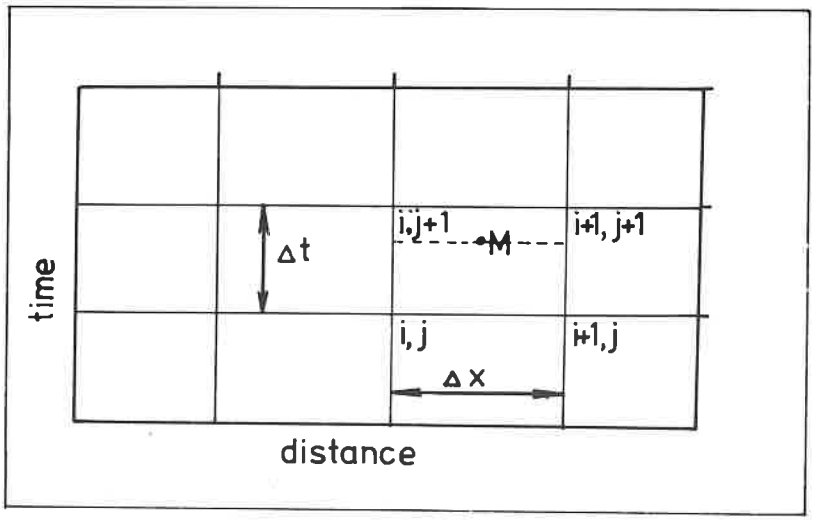

Figure 9. Network of points on x, t - plane.

$$\frac{1}{2\Delta t}(Q_{i+1}^{j+1} - Q_{i+1}^{j} + Q_{i}^{j+1} - Q_{i}^{j}) + \frac{\theta}{\Delta x}\left[(\beta\frac{Q^2}{A})_{i+1}^{j+1}\right.$$

$$\left. - (\beta\frac{Q^2}{A})_{i}^{j+1}\right] + \frac{(1-\theta)}{\Delta x}\left[(\beta\frac{Q^2}{A})_{i+1}^{j} - (\beta\frac{Q^2}{A})_{i}^{j}\right]$$

$$+ g\hat{A}\left\{\left[\frac{\theta}{\Delta x}(y_{i+1}^{j+1} - y_{i}^{j+1}) + \frac{(1-\theta)}{\Delta x}(y_{i+1}^{j} - y_{i}^{j})\right]\right.$$

$$\left. + \hat{S}_f\right\} - v_x\hat{q} = 0 \qquad (48b)$$

In equations (48a) and (48b) the variables $\hat{b}$, $\hat{A}$, $\hat{S}_f$ and $\hat{q}$ are expressed as follows:

$$\hat{b} = \frac{\theta}{2}(b_{i+1}^{j+1} + b_{i}^{j+1}) + \frac{(1-\theta)}{2}(b_{i+1}^{j} + b_{i}^{j}) \qquad (48c)$$

$$\hat{A} = \frac{\theta}{2}(A_{i+1}^{j+1} + A_{i}^{j+1}) + \frac{(1-\theta)}{2}(A_{i+1}^{j} + A_{i}^{j}) \qquad (48d)$$

$$\hat{S}_f = \frac{\theta}{2}\left[(S_f)_{i+1}^{j+1} + (S_f)_i^{j+1}\right] + \frac{(1-\theta)}{2}\left[(S_f)_{i+1}^{j} + (S_f)_i^{j}\right] \quad (48e)$$

$$\hat{q} = \theta q_{i+\frac{1}{2}}^{j+1} + (1-\theta) q_{i+\frac{1}{2}}^{j} \quad (48f)$$

In equations (48) $q_{i+\frac{1}{2}}$ is the lateral flow between nodal points i and i+1.

In equations (48a) and (48b) all the variables with superscript j are known and all the variables with superscript (j+1) are unknowns. Eqs. (48a) and (48b) contain only four independent variables, namely the values of the discharge and stage at grid points (i,j+1) and (i+1,j+1). It is also worth mentioning that the discharge increment and the time increment need not be constants.

Eqs. (48a) and (48b) constitute a system of two nonlinear algebraic equations in four unknowns. By themselves they are not sufficient to evaluate the unknowns. However, a solution can be obtained by considering all N points along the x axis simultaneously. In this way a total of 2(N-1) equations with 2N unknowns may be written by applying (48a) and (48b) recursively to the N-1 rectangular grids along the x axis. Two additional equations are required for the system of equations to be determinate. These equations are available from the boundary conditions.

The boundary conditions consist of a description of either water surface elevation y or discharge Q as a function of time at the upstream and downstream boundaries. The downstream boundary condition may also be a known relationship between stage and discharge. The boundary conditions can be expressed as follows:

$$F_0(y_1, Q_1) = 0 \quad (49a)$$

$$F_N(y_N, Q_N) = 0 \tag{49b}$$

Equations (48a) and (48b) can be written as follows:

$$F_i\ (y_i, Q_i, y_{i+1}, Q_{i+1}) = 0 \tag{50a}$$

$$G_i\ (y_i, Q_i, y_{i+1}, Q_{i+1}) = 0 \tag{50b}$$

Eqs. (49)-(50) simulate the boundary conditions and the equations of motion for flow through a channel reach. A system of 2N nonlinear algebraic equations for the solution of 2N unknowns can be expressed as follows:

$$\begin{aligned} &F_o\ (y_1, Q_1) = 0 \\ &F_1\ (y_1, Q_1, y_2, Q_2) = 0 \\ &G_1\ (y_1, Q_1, y_2, Q_2) = 0 \\ &\qquad\vdots \\ &F_N\ (y_N, Q_N) = 0 \end{aligned} \tag{51}$$

Owing to the nonlinearity of the system, it is necessary to use an iterative procedure to obtain a solution. The generalized Newton iteration method /2/ has been found to be very suitable for open channel flows. In this method, the solution of the nonlinear system of equations is reduced to successive solutions of linear systems. However, each system has a banded sparse coefficient matrix and a specialized direct method proposed by Fread /10/ is used for solving a system of linear equations.

The SATT-I model will be extended so that transient flows can be taken into account. An automatic calibration routine for finding the roughness coefficients will also be programmed soon.

2.52 Channel routing by the Muskingum method

When the SATT-I model is used as a prediction tool, the channel routing method should be as simple as possible. The Muskingum method was selected. The equations used have been written in (39)-(42).

The parameters x and k can be calibrated with all available data. The use of simplified equations may, however, lead to difficulties in practice, most often because of one of two factors: developments in the river basin and the limited range of applicability of simplified methods. Simplified methods are predictive only as long as the inputs stay within the range for which the model has been calibrated, and as long as the system itself does not change. The above difficulties in application of the Muskingum method can be avoided by a three-step strategy:

(i) First a detailed model based on the full de St Venant equations is built, and is calibrated with all available data. The complete calibrated model allows not only for the simulation of exceptional unrecorded events beyond the range of calibration, but also for the inclusion of river system modifications such as dams, dykes etc., without the loss of its predictive capacity.

(ii) The coefficients of the Muskingum method are calibrated by repeated use of the full model (the simulation results of the complete model are used as "measurements").

(iii) The Muskingum method is implemented on the computer for real-time forecasting purposes.

2.53 Lake routing

The routing of flow through natural lakes is based on free-flow conditions, i.e., elevation-outflow relationships are fixed, and outflow is determined by hydraulic head. Routing is accomplished by an iterative solution of the storage equation.

$$2S_2/\Delta t + O_2 = I_1 + I_2 + 2S_1/\Delta t - O_1 \qquad (52)$$

This routing process is illustrated in Fig. 10. The initial estimate of outflow (O_2) is assumed to equal the outflow at the beginning of the period (O_1). An outflow value Q_T is then determined by solution of the storage equation, and according to elevation-storage relationships that are entered into the computer in table form. The Q_T value is then tested and the process repeated until an acceptable outflow is obtained.

2.6 Regulation routines of reservoirs and lakes

The SATT-I program is composed of a main program and several subroutines. The subroutines are independent of the particular water area under consideration. The object area is described in the main program with pertinent data such as the number and size of reservoirs and lakes, area subdivisions, river stretches, engineering measures such as straightening of river beds, areas exposed to floods, embankments, etc. The various parts of the program can be freely combined; this permits its adaptation to all types of watercourse. For instance, there is no upper limit for the number of reservoirs in the program.

The model has two main alternatives for the use of regulation reservoirs:

1) Intention to reach the reservoir's lower regulation limit before the spring flood which is used to fill it up again.
2) The user may freely set target values for the water level in or releases from the reservoirs.

In alternative 2, an option can be made between three different policies of water release:

a) the water level is maintained constant,
b) a goal is set for the the amount of release,
c) a goal is set for the level of water.

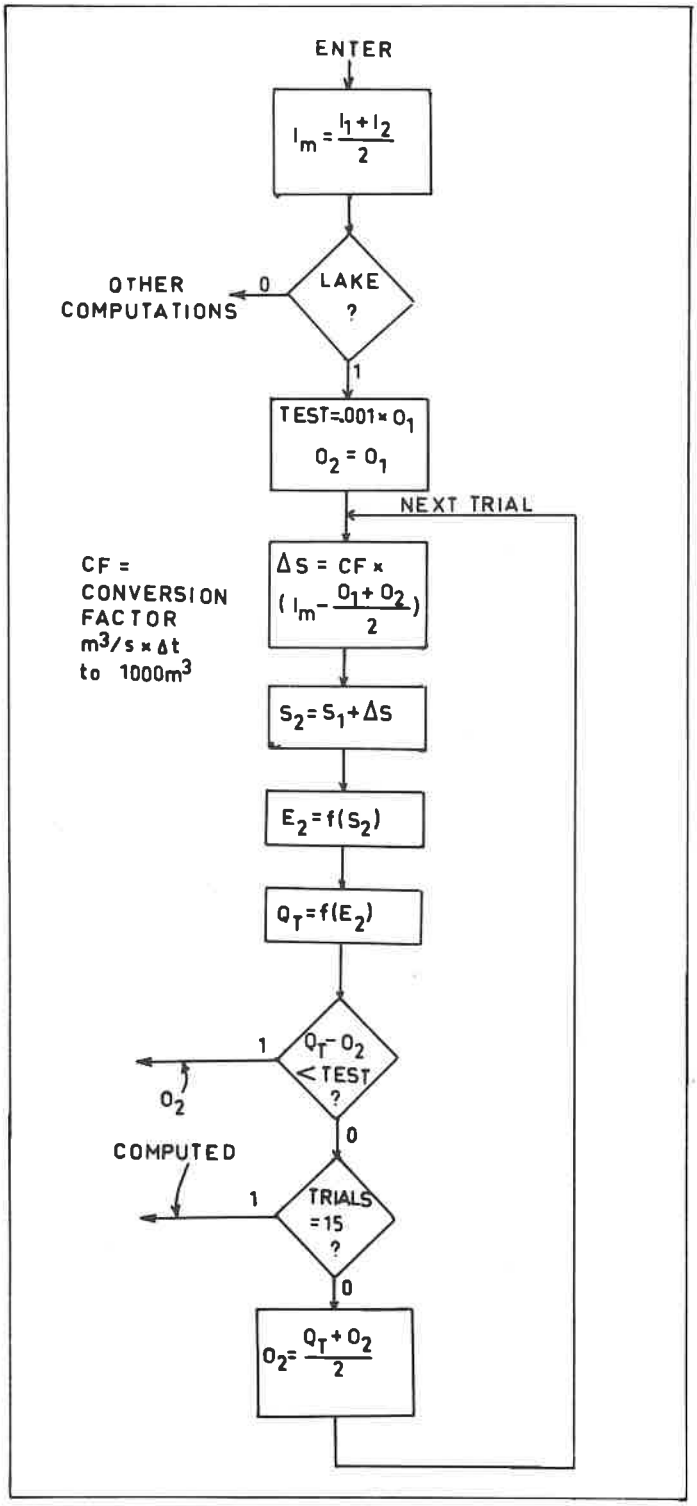

Figure 10. Lake routing technique used in SATT-I model.

3 CALIBRATION

3.1 Parameter values

The 10 calibrable parameters included in the SATT-I model are shown in Table 1.

The most common procedure used for the calibration of rainfall-runoff models is the Rosenbrock method, or a modification of it (e.g. /25/). Also the simplex algorithm developed by Nelder and Mead (ref. /27/) has been applied in various models and by several authors (e.g. /12, 29/. Manley /22/ has examined the application of both the Rosenbrock method and the simplex algorithm to one and the same model and the same input data. According to Manley, there is no essential difference between the results obtained by the use of these two methods.

The parameters of the SATT-I program are calibrated using the simplex algorithm. Since automatic calibration requires a relatively large computer capacity, it was necessary to develop a separate calibration program called KALIB. This program is used for determining the most appropriate parameter values for each catchment area; these values are then transferred directly to the input of the SATT-I program. Thus the rainfall-runoff model processed on a microcomputer only includes the adaptive calibration system described in paragraph 3.2.

3.2 Adaptive calibration system

The SATT-I model includes a custom-developed adaptive calibration system which is aimed at correcting the forecasts produced by the model. The adaptive calibration makes it possible to diminish forecasting errors due to the following factors, among others:

- calculation of snowmelt rate by a method based on mean temperature only
- the effect of frost on hydraulic conductivity
- errors in the measurement of precipitation

Table 1. Calibrable parameters of the SATT-I model and their probable range of variation.

Parameter	Symbol	Range of variation
Snowmelt parameter	R	2.0...3.5 mm/°C/d
Parameter for snow-free ground	L_{limit}	20...60 mm
Maximum surface storage	SURFM	10...50 mm
Percolation from surface storage	UPERKO	0.1...1.0 mm/d
Hydraulic conductivity of saturated soil	K_S	15...100 mm/d
Limit value for surface storage	$BSTO_L$	10...35 mm
Coefficient in equation (37)	a	0.005...0.015
Coefficient in equation (38)	b	0.10...0.35
Parameter in the Muskingum method	k	0.5...4.0 d
Shape factor, Muskingum method	X	0.01...0.50

The purpose of the adaptive calibration system is the same as that of the Kalman filter /16, 17, 24, 26/. Both methods use discharge observations which are as recent as possible and which serve for changing the model parameters or the state equation so as to bring the discharge calculated by the model as close to reality as possible. In other words, the calculation procedure must be true to the actual "runoff history".

The adaptive calibratiron system of the SATT-I model is much simpler than the Kalman filter technique. The objective is to find such values for two parameters - the snowmelt parameter R and the parameter V_{MIN} (equation (31)) - that the daily observed and calculated discharges differ from each other at most by the amount ΔQ. The magnitude of ΔQ is estimated, for instance, according to the reliability of the discharge curve belonging to the observation point. Generally, ΔQ varies between 5 to 10 per cent of the amount of the observed discharge.

If the absolute value of difference between the observed discharge and the calculated discharge on some day is greater than ΔQ, then the values of the parameters R and V_{MIN} are changed so that the absolute difference is equal to ΔQ at the most. The adaptive calibration is inoperative on days when

- the mean temperature is lower than the base temperature T_B (i.e. no melting of snow occurs)
- no precipitation occurs and the catchment area is free of snow.

Thus, under the above circumstances, the discharge calculated by the model cannot be corrected. When forecasting a spring flood, for instance, the adaptive calibration works through the appropriate modification of the parameters R and V_{MIN} each time a new discharge observation is received, permitting to adapt the moment of forecast as close to the real situation as possible.

The adaptive calibration of the SATT-I program makes it possible to manipulate the summertime forecasting errors which are due to the inaccuracy of rainfall measurements. To achieve the corrective function, the program modifies the distribution of the given precipitation over the catchment area (the amount of precipitation is not changed). The distribution of rainfall is effected so that a certain part of it ($=A_{SV}P$) may cause surface runoff from the surface storage while the other part Q_{soil} ($= (1 - A_{SV})\ P$) is assumed to get infiltrated into the non-saturated zone, provided that the infiltration capacity calculated from formula (16) is not smaller than Q_{soil}. In the event that the calculated discharge some day differs from the observed discharge by more than ΔQ, the program will either increase or decrease the proportion of precipitation ending up in the surface storage. The value of A_{SV} is left unchanged (A_{SV} = proportion of poorly conductive or impervious soil surface in the catchment area; in practice, this proportion generally consists of the whole area of lakes and clayey cultivated lands within the catchment area).

4 PRACTICAL APPLICATION TO THE KYRÖNJOKI RIVER BASIN

4.1 Discription of the area

Owing to some controversial flood control projects carried out in the area, the Kyrönjoki river basin (Fig. 11) in Western Finland has been the most disputed watercourse in the country during the past decade. In particular, the operation policy of flood control reservoirs has become a bone of contention since there have been claims that it is too closely geared to the sole interests of hydroelectric power companies. Disagreement also reigns over the hydrological effects of the embankments and the straightening channel planned for protecting the flood-prone area of Munakka near the city of Seinäjoki. This area is very much exposed to floods (in spring, as much as 7000 ha of the area can become flooded).

The total area of the Kyrönjoki basin is 4920 km^2. The percentage of cultivated lands is 24.4 %, forests 47.2 %, peatland 26.0 %, water area 0.9 %, and other areas 1.5 %. The basin is rather flat, the average inclination being 2 %. The annual temperature mean is 3.2 ^{o}C, annual precipitation 610 mm, annual runoff 280 mm, and annual evaporation 330 mm. The annual maximum of the water equivalent of snow is 85 mm on the average.

In concequence of the small number of lakes in the area, discharge in Kyrönjoki river varies considerably. At the Munakka gauging point the difference between the observed maximum and minimum is about 6.5 m. Characteristics of the flood control reservoirs used in the area are shown in Table 2.

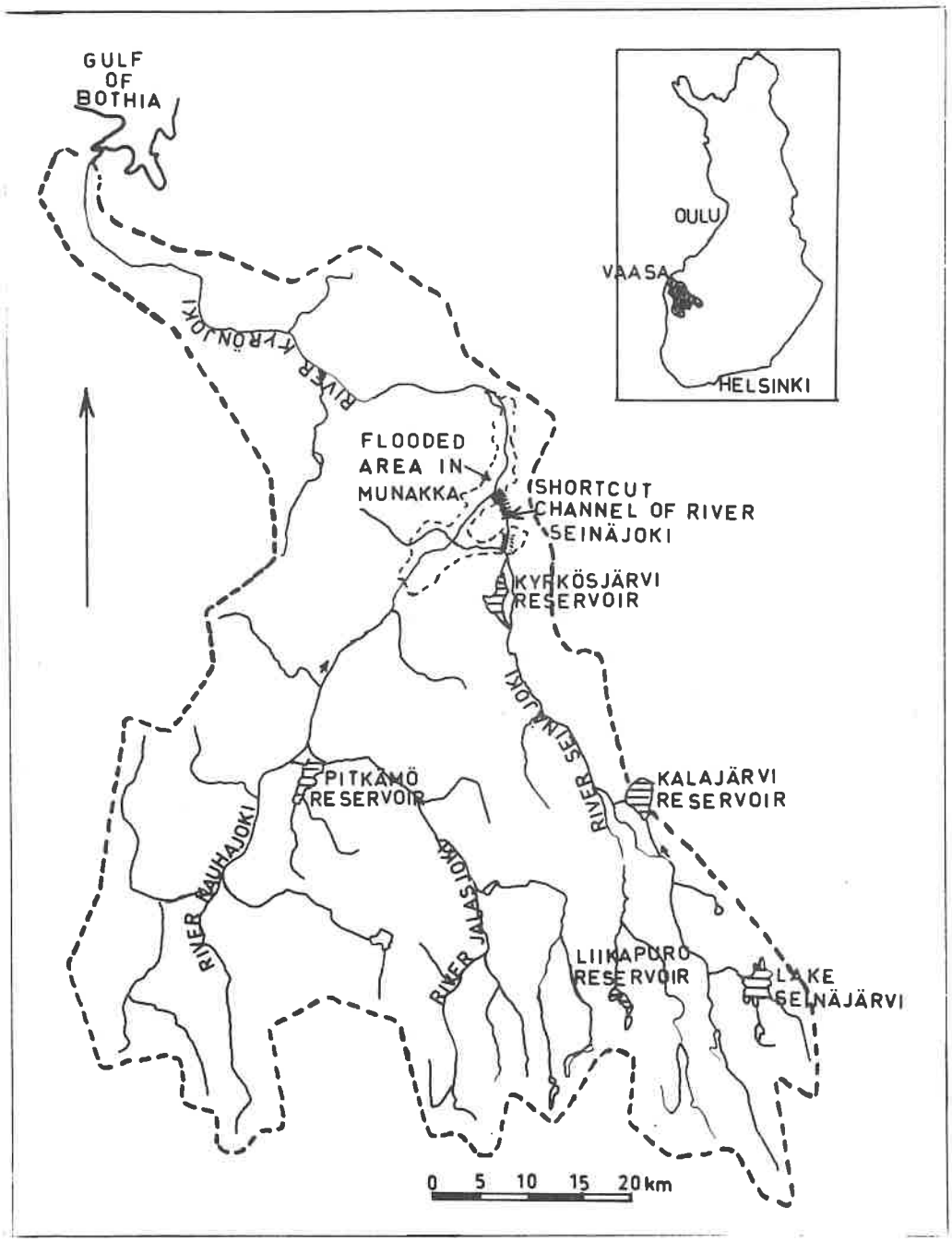

Figure 11. The Kyrönjoki river basin.

Table 2. Characteristics of the flood control reservoirs and lakes of the Kyrönjoki river basin.

Lake/ reservoir	Area ha	Storage $10^6 m^3$	Drainage area km^3
Kalajärvi	1150	42.0	512
Kyrkösjärvi	880	11.0	820
Pitkämö	100	7.0	2116
Seinäjärvi	880	11.0	99
Liikapuro	310	5.3	27

4.2 Use of the model for forecasting purposes

The simple adaptive calibration feature of the SATT-I model has proved to be quite well suited to making short-term discharge forecasts; this is due to the fact that it permits bringing the calculated discharge into a close correspondence with the values of observed discharge. As an example, Fig. 12 shows the forecasting of readings on the Munakka gauge in spring 1971. In practice, these forecasts are based on weather forecasts received from the Institute of Meteorology. However, for more simplicity, the actual temperature and precipitation observations are used as input data in our example. Forecasting the discharge in spring 1971 was exceptionally difficult because of the deep penetration of frost. In years like this, the model's calibration system is particularly useful as it continually corrects the forecasts according to new observations entered into the program.

In summertime, forecasting the discharge is more difficult than in spring because there are only four precipitation gauges available for the calculation of areal rainfall. The adaptive calibration system, which during summer periods modifies the areal distribution of rainfall, has again proved efficient here (Fig. 13).

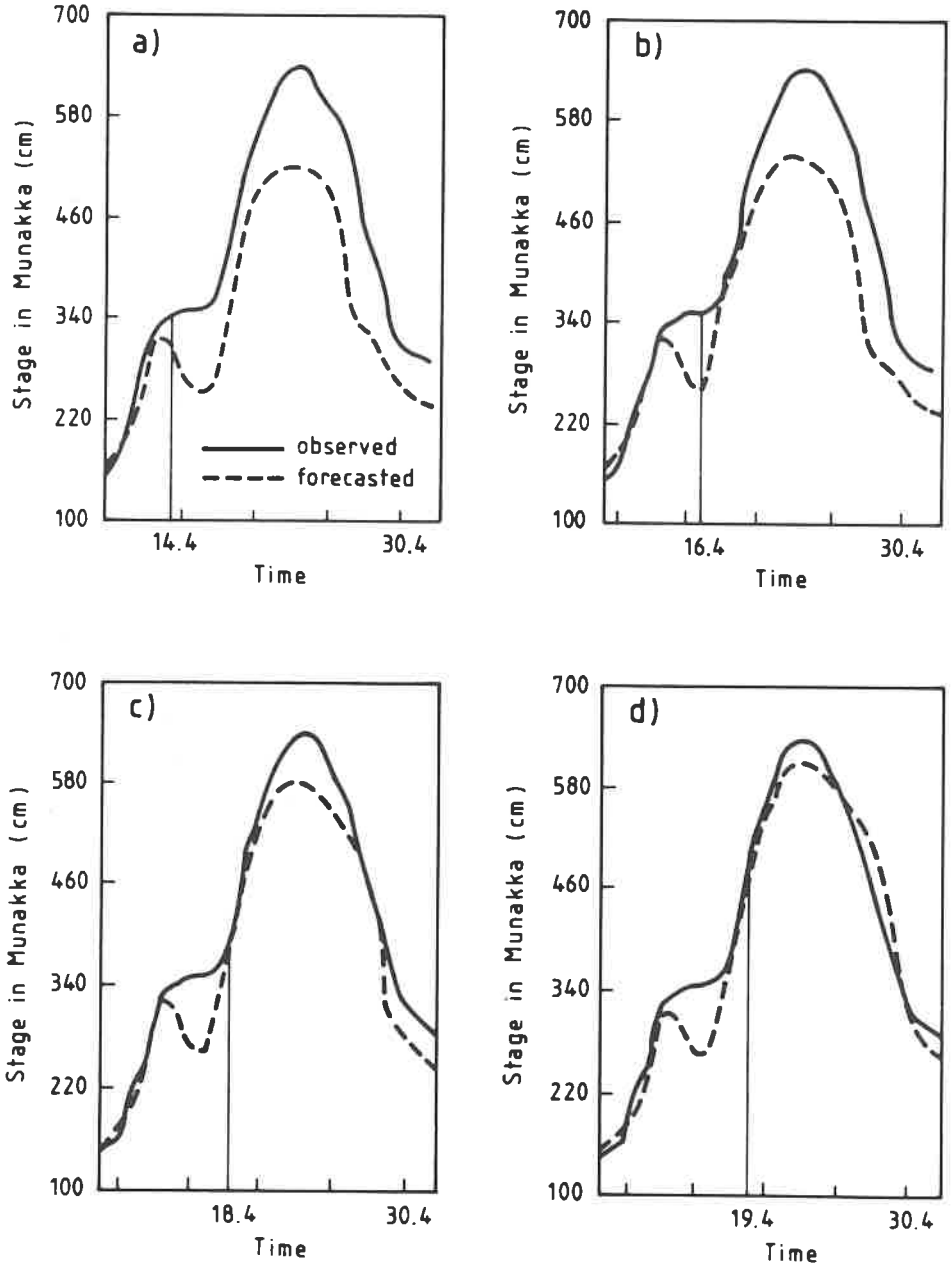

Figure 12. Forecasting of readings on the Munakka gauge in spring 1971 by using SATT-I model. Discharge measurements available up to
a) 14.4
b) 16.4
c) 18.4
d) 19.4.

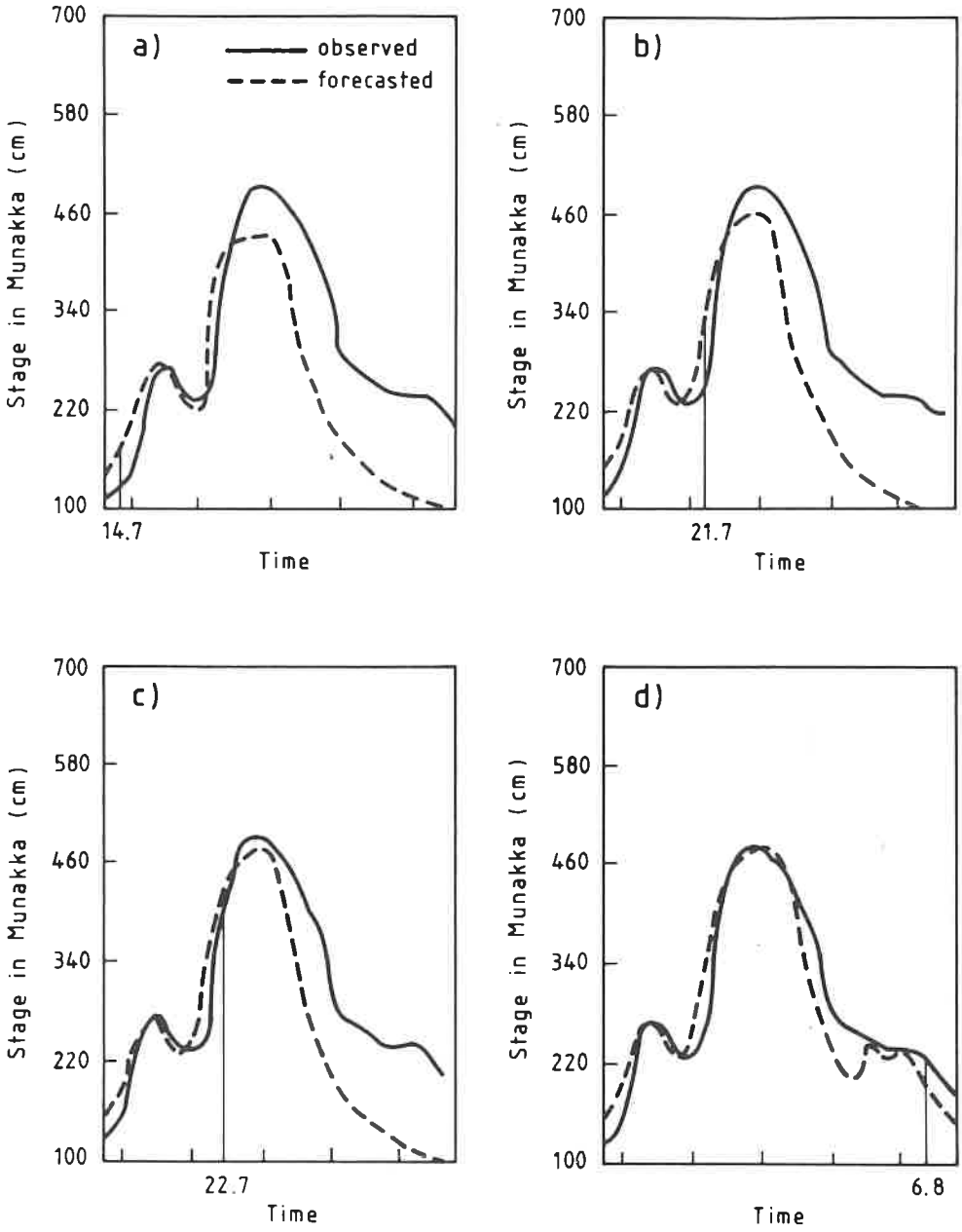

Figure 13. Forecasting of readings on the Munakka gauge in summer 1979 by using SATT-I model. Discharge measurements available up to
a) 14.7
b) 21.7
c) 22.7
d) 6.8

4.3 Use of the model in hydrological planning

As an example of the model's application to planning purposes, Fig. 14 shows a study on how the flood control reservoirs should be operated in order to even out the flood peak occurred in summer 1979. This particular flood caused considerable losses to local farmers and touched off an incisive debate in the press about the ability and determination of the National Board of Waters to properly carry out the regulation of the river. The control reservoirs were almost full when the rains began which were to cause the flood.

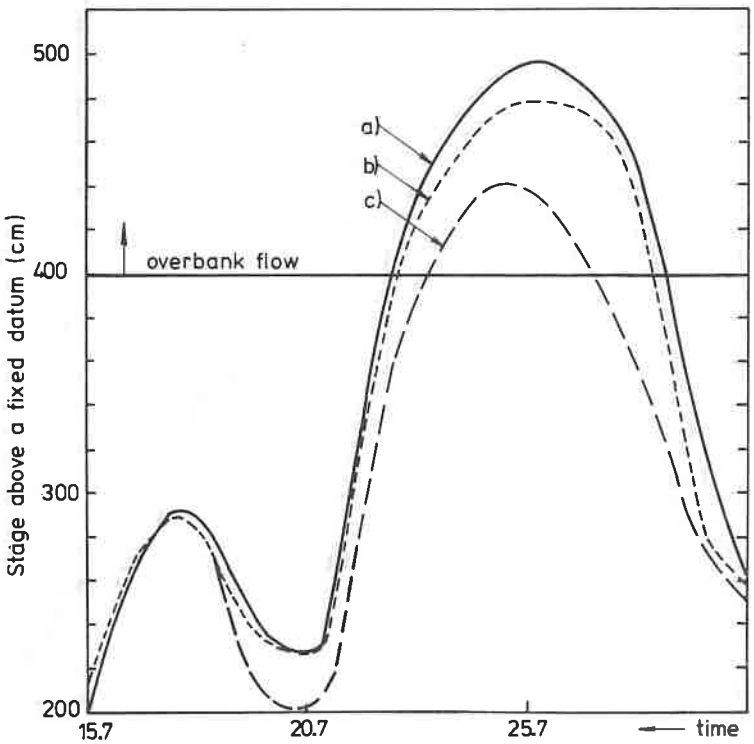

Figure 14. Readings on the Munakka gauge in the Kyrönjoki river basin during summerflood of 1979.
a) Measured stages
b) The reducing effect of the reservoirs on the flood if their water level had been at the lower summertime limit just before the flood
c) The reducing effect of the reservoirs on the flood if their water level had been at the minimum wintertime limit just before the flood.

By decision of the Court of Water Rights, the regulation ranges established for the reservoirs are rather narrow during the summertime. The difference between the permitted lower and upper water levels in the Pitkämö reservoir is only 0.5 to 1.0 m depending on the date, in the Kyrkösjärvi reservoir the regulation range is only 0.35 m and in the Kalajärvi reservoir 0.50 m. Thus it is obvious that the reducing effect of the reservoirs on the flood would not have been significant even if their water level had been at the lower summertime limit just before the flood. The Court of Water Rights has established the following allowable maximum differences between the upper limit and the wintertime minimum in the reservoirs: Pitkämö 10.00 m, Kyrkösjärvi 2.00 m, and Kalajärvi 6.50 m. These limits lead us to the conclusion that even if the reservoirs would have been at their wintertime minimum water level before the heavy rain started, the flood could not have been avoided completely; however, the extension of the flooded area would have been essentially smaller and the duration of the flood shorter. This is due to the fact that 70 to 80 per cent of the discharge in the Munakka flood area originates from that part of the watercourse where there is only one regulation reservoir, namely Pitkämö.

Apart from the current situation in the area, the SATT model also discribes an alternative in which approximately 30 per cent of the flood area is protected by embankments and the waters of river Seinäjoki are diverted from the area along a shortcut channel (Fig. 11). In addition, the user of the program has the option of calculating discharge and water stages in the flood area while the watercourse is in its natural state. The results of the calculations based on these alternatives and the summer flood of 1979 are shown in Table 3.

Table 3. The results of the calculations based on the summer flood of 1979.

Date	Q_C	Q_F	Q_N	W_C	W_F	W_N
13.7	22	22	22	33.57	33.57	33.57
14.7	26	26	26	33.68	33.68	33.68
15.7	43	43	43	34.18	34.18	34.18
16.7	65	65	65	34.71	34.71	34.71
17.7	75	75	75	34.93	34.93	34.93
18.7	63	63	63	34.67	34.67	34.67
19.7	51	51	51	34.37	34.37	34.37
20.7	49	49	51	34.31	34.41	34.37
21.7	81	81	88	35.07	35.07	35.20
22.7	126	132	140	35.90	36.00	36.12
23.7	159	177	171	36.42	36.68	36.61
24.7	177	201	189	36.68	36.99	36.83
25.7	184	192	200	36.77	36.87	36.98
26.7	182	167	196	36.74	36.54	36.92
27.7	170	140	181	36.59	36.13	36.72
28.7	129	114	147	35.95	35.70	36.24
29.7	71	83	67	34.84	35.11	34.75
30.7	62	62	62	34.63	34.63	34.63
31.7	45	45	45	34.23	34.23	34.23
1.8	39	39	39	34.07	34.07	34.07

Q is discharge (m^3/s) in the Kyrönjoki river at Seinänsuu

W stage (m) in the Kyrönjoki river at Seinänsuu

C sub-index denoting the current situation

F sub-index denoting the situation when 30 per cent of the flood area in Munakka is protected by embankments and the waters of river Seinäjoki are diverted along the shortcut channel

N sub-index denoting the natural state

5 DISCUSSION

It can be concluded that the SATT-I model largely fulfils the requirements set at the beginning of its development work. The model's structure enables it to be applied to all types of watercourse, it is easy to use and can be run on both large and small computers. The processes included in the model are all based on physical principles. The required input data consist of generally-measured hydrological quantities; the model can be used for both forecasting purposes and the calculation of hydrological effects caused by water regulation and construction schemes. The model incorporates versatile calculation routines for flood control reservoirs.

The simple adaptive calibration has proved quite effective. Karvonen /14/ used with good results a carefully calibrated and verified SSARR model for forecasting the spring flood of 1980. However, the results obtained by the same model for spring 1981 were unsatisfactory (Fig. 15a). The ability of the SATT-I model to continually correct the forecasts with new observation data clearly leads to a better result (Figs. 15b... 15d). This is why, in further development of the model, the main emphasis will henceforth be laid on the adaptive calibration. The preparation of a new calibration system using the Kalman filter technique is currently under way.

Naturally the accuracy of the model cannot exceed of that of the observation data on which it is based. A closer look at the situation in spring 1981 gives a better idea of the difficulties involved in measuring the water balance in the Kyrönjoki catchment area. On the first day of April the water equivalent of snow had reached 165...170 mm, and the areal rainfall for April and May was 31 mm. For the same period, the measured runoff was 202 mm; the amount of 15 mm was stored in reservoirs. Now if evaporation is estimated at 70 mm, the change in soil water storage ought to be as much as 90 mm in order to comply with the water balance equation. There is a reason to doubt that a change of this magnitude could not occur in the soil.

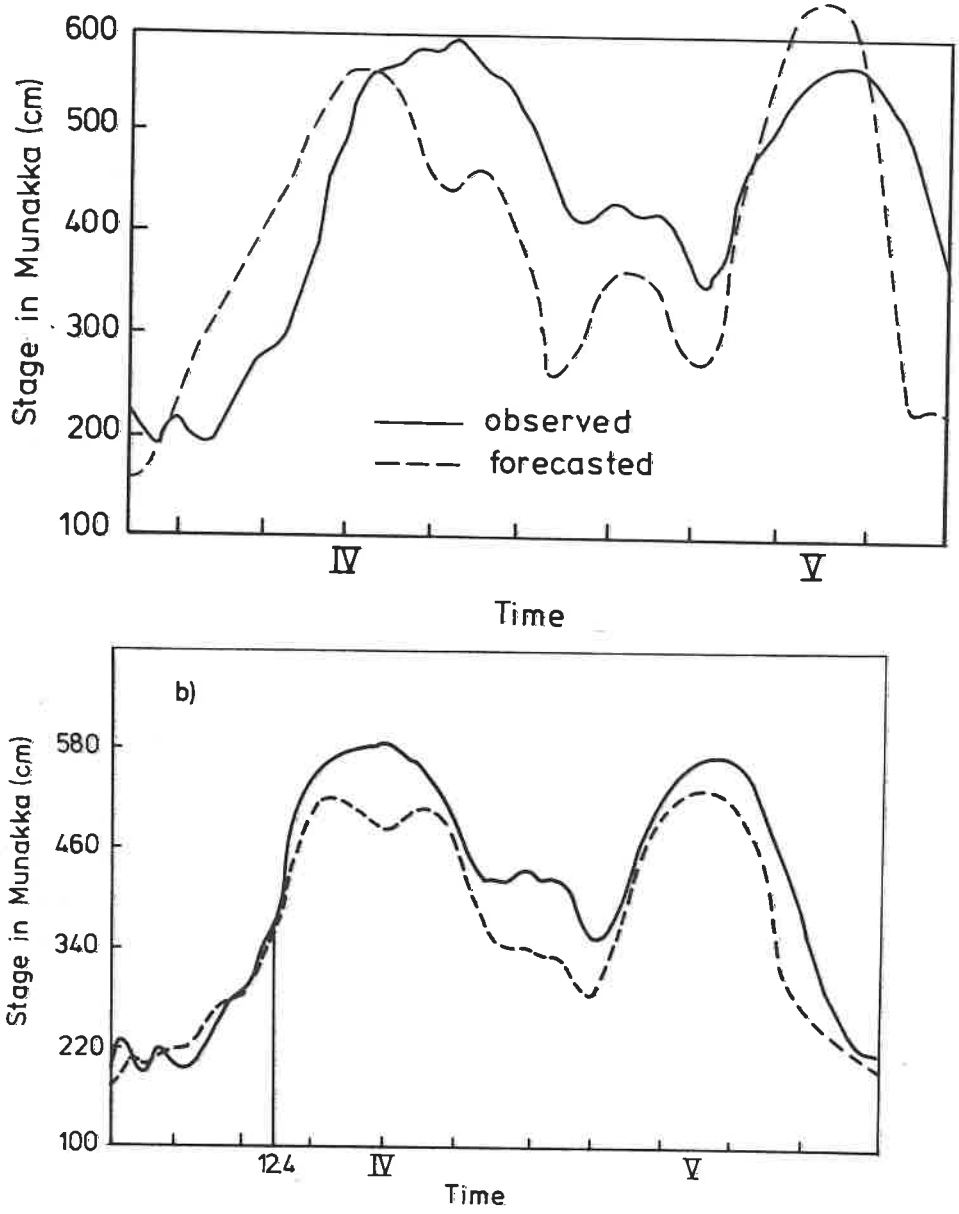

Figure 15. Forecasting of readings on the Munakka gauge in spring 1981.
a) Using SSARR model
b) Using SATT-I model when discharge measurements were available up to 12.4

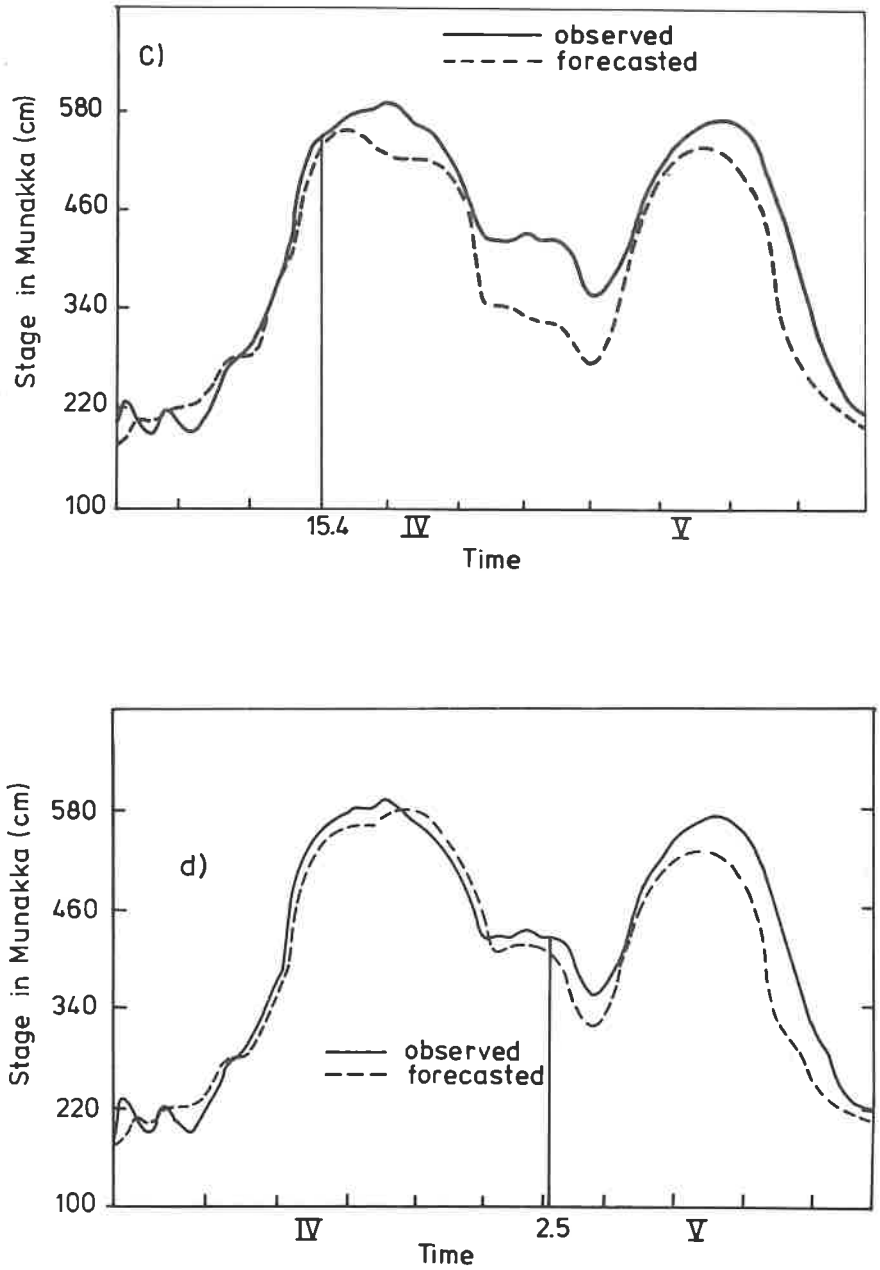

Figure 15. Forecasting of readings on the Munakka gauge in spring 1981.
c) Using SATT-I model when discharge measurements were available up to 15.4
d) Using SATT-I model when discharge measurements were available up to 2.5

It is probable that this deviation from the water balance equation can be explained mainly by errors in the measurement of snow storage, precipitation and runoff. A network of only four precipitation gauging stations is quite insufficient for a proper determination of areal precipitation. Increasing the number of precipitation gauges or the use of a precipitation radar are indispensable conditions for an accurate forecasting of discharge especially in summertime.

6 SUMMARY

The SATT-I model is a rainfall-runoff model designed to simulate the movement of water in a catchment area in a manner which is as physical as possible. Thus the calculation of soil moisture is based on numerical solution of the continuity equation and the Richards equation. Similarly, the advence of discharge in the watercourse is calculated numerically from St. Venant's equations. Recent studies on the formation of runoff have been taken into account in the model. Mathematical expressions have been developed to assess the effect of frost on runoff. If the input data collected on the catchment area are insufficient for the use of the soil moisture model, changes in soil water storage can be treated in a conceptual way. The propagation of floodwave can optionally be determined using the Muskingum method. This method is also used in the timing of direct runoff.

The calculation routines for lakes and reservoirs have been designed with the objective of making them applicable to all practical cases. The use of the St. Venant's equations makes it possible to include the daily regulation of river streamflow in the calculation.

The model has 10 calibrable parameters whose values are determined with the aid of an automatic calibration program using a simplex algorithm. The probable variation ranges of these parameters are given in the text. The model is provided with an adaptive calibration system which is aimed at improving the accuracy of forecasts in proportion as new observation data are received.

The working principle of the adaptive calibration is very simple. When forecasting springtime floods, the values of the snowmelt rate parameter and the parameter expressing the relative hydraulic conductivity of soil are modified on-line in the model every day until the difference between the values of calculated and measured discharge falls within preset limits depending upon the accuracy of measurement. In summertime, the

distribution of areal precipitation over the catchment area is proportioned out between hydraulically conductive and non-conductive partial areas in a way which permits achieving satisfactory results.

The use of the SATT-I model is exemplified by its sample application to the Kyrönjoki river basin for forecasting the amount of discharge and the development of water level resulting from different policies of regulation; the effect of various water engineering schemes on runoff and water level are also studied and compared with each other.

ACKNOWLEDGEMENTS

The authors are sincerly indebted to Mr J. Saavalainen, managing director of Finnish Drainage Centre for his support during the work. We warmly thank Ms. K. Rousu for her patience while typing the manuscript.

Manuscript received 28 May, 1982

REFERENCES

1. Amein, M., An implicit method for numerical flood routing: Water Resources Research 4 (1968)4, p. 719-726.
2. Amein, M. and Fang, C.S., Implicit flood routing in natural channels. Journal of the Hydraulics Division 96 (1970) HY12, p. 2481-2500.
3. Andersson, S. and Wiklert, P., Markfysikaliska undersökningar i odlad jord XXIII. Om de vattenhållande egenskaper hos svenska jordarter. Grundförbättring (1972)25, p. 53-143.
4. Bellmans, C., Wesseling, J.G. and Feddes, R.A., Simulation model of the water balance of a cropped soil providing different types of boundary conditions (SWATRE). ICW. Nota 1257. Unpublished.
5. Bergström, S. and Forsman, A., Development of a conceptual deterministic rainfall-runoff model. Nordic Hydrology 4 (1973)2, p. 147-170.
6. Bloemen, G.W., Calculation of hydraulic conductivities of soils from texture and organic matter content. Z. Pflanzenernaehr. Bodenkd. (1980)143, p. 581-605.
7. Cunge, J.A., Holly, F.M. and Wervey, A., Practical aspects of computational river hydraulics. 1. Edition. London, Pitman Publishing Limited, 1980.
8. Dincer, T., Payne, B.R., Florkowski, T., Martinec, J. and Tongiorgi, E., Snowmelt runoff from measurements of tritium and oxygen-18. Water Resources Research 6 (1970)1, p. 114-123.
9. Feddes, R.A., Kowalik, P.J. and Zaradny, H., Simulation of field water use and crop yield. 1. Edition. Wageningen, 1978.
10. Fread, D.L., Discussion of implicit flood routing in natural channels. Journal of the Hydraulics Division 97 (1971)HY7, p. 1156-1159.
11. Garrison, J.M., Granju, J-P.P. and Price, J.T., Unsteady flow simulation in rivers and reservoirs. Journal of the Hydraulics Division 95(1969) HY5, p. 1559-1575.
12. Johnson, P.R. and Pilgrim, D.H., Parameter optimization for watershed models. Water Resources Research 12 (1976)3, p. 477-486.

13. Kaitera, P. and Teräsvirta, H., Snow evaporation in south and north Finland 1969/70 and 1970/71. Aqua Fennica (1972), p. 11-19.

14. Karvonen, T., Sadanta-valuntamallin soveltaminen Kyrönjoen vesistösuunnitteluun. Vesihallituksen monistesarja (1980)28.

15. Keränen, J., Über den Bodenfrost in Finnland. Suomen Valtion Meteorologisen Keskuslaitoksen toimituksia (1923)12.

16. Kitanidis, P.K. and Bras, L.R., Real-time forecasting with a conceptual hydrologic model, 1, Analysis of uncertainty. Water Resources Research 16 (1980)6, p. 1025-1033.

17. Kitanidis, P.K. and Bras, L.R., Real-time forecasting with a conceptual hydrologic model, 2, Application and results. Water Resources Research 16 (1980)6, p. 1034-1044.

18. Kuusisto, E., Konseptuaalisten valuntamallien soveltamisesta Suomessa. Vesitalous 18 (1977)1, p. 16-20.

19. Kuusisto, E., Suur-Saimaan vesitase ja tulovirtaaman ennustaminen. Vesientutkimuslaitoksen julkaisuja 19 (1978)26.

20. Liggett, J.A., Mathematical flood determination in open channels. Journal of Engineering Mechanics Division 94 (1968)EM4, p. 947-963.

21. Liggett, J.A. and Woolhiser, D.A., Difference solutions of the shallow-water equation. Journal of Engineering Mechanics Division 95 (1967)EM2, p. 39-71.

22. Manley, R.E., Calibration of hydrological model using optimization technique. Journal of the Hydraulics Division 104 (1978)HY2, p. 189-201.

23. Martinec, J., Subsurface flow from snowmelt traced by tritium. Water Resources Research 11 (1975)3, p. 496-498.

24. Moore, R.J. and O'Connel, P.E., Real-time forecasting of flood events using transfer function noise models, Part 1. Wallingford, Institute of Hydrology, 1978.

25. O'Connel, P.E., Nash, J.E. and Farrell, J.P., River flow forecasting through conceptual models, Part II - The Brosna Catchment at Ferbane. Journal of Hydrology 10 (1972), p. 317-329.
26. O'Connell, P.E. (editor),Real-time hydrological forecasting and control (Proc. 1st. International Workshop, July 1977). Wallingford, Institute of Hydrology, 1980.
27. O'Neill, R., Algorithm AS 47. Function minimization using a simplex procedure. Applied Statistics 20 (1971), p. 338-345.
28. Ponce, V.M. and Yevjevich, V., Muskingum-Cunge method with variable parameters. Journal of the Hydraulics Division 104 (1978)HY12, p. 1663-1671.
29. Porter, J.W. and McMahon, T.A., A model for simulation of streamflow from climatic records. Journal of Hydrology 13 (1971), p. 297-324.
30. Remson, I., Hornberger, G.M. and Molz, F.J., Numerical methods in subsurface hydrology. New York, Wiley Interci., 1971.
31. Rohde, A., Spring flood, meltwater or ground-water? Nordic Hydrology 12 (1981), p. 21-30.
32. Sklash, M.G. and Farvolden, R.N., The role of groundwater in storm runoff. J. of Hydrology 43(1979), p.45- 65.
33. USCE., Engineering and design runoff from snowmelt. Washington, U.S. Government Printing Office, 1960.
34. USCE., SSARR model: Program description and users manual. Oregon, North Pasific Division, 1975.
35. Vakkilainen, P., Vesitasemallien kehittäminen vesien käytön suunnittelua varten. Loppuraportti Suomen Akatemialle. TKK:n vesitalouden laboratorion monistesarja. Otaniemi, 1981.
36. Vakkilainen, P., Maa-alueelta tapahtuvan haihdunnan arvioinnista (On the estimation of evapotranspiration). Acta Universitatis Ouluensis, Series C Technica N:o 20. Oulu, Oulun yliopisto, 1982.
37. Vakkilainen, P. and Karvonen, T., SSARR, sadanta-valuntamalli vesistöjen optimaalisen suunnittelun ja käytön pohjaksi ? Vesitalous 21 (1980) 2, p. 36-44.

38. Virta, J., Sadanta-valuntamalli ja sen soveltaminen. Geofysiikan päivät 10.-11.3.1977. Helsinki, Geofysiikan seura, 1977.